THE ASTRONOMICAL JOURNAL, 119:2428–2436, 2000 May

A REDETERMINATION OF THE MASS OF PROCYON

T. M. GIRARD,[1] H. WU,[1] J. T. LEE,[1] S. E. DYSON,[1] W. F. VAN ALTENA,[1] E. P. HORCH,[2] R. L. GILLILAND,[3]
K. G. SCHAEFER,[3,4] H. E. BOND,[3] C. FTACLAS,[5] R. H. BROWN,[6] D. W. TOOMEY,[7]
H. L. SHIPMAN,[8] J. L. PROVENCAL,[8] AND D. POURBAIX[9]
Received 1999 October 29; accepted 2000 January 27

ABSTRACT

The parallax and astrometric orbit of Procyon have been redetermined from PDS measurements of over 250 photographic plates spanning 83 years, with roughly 600 exposures used in the solution. These data are combined with two modern measurements of the primary–white dwarf separation, one utilizing a ground-based coronagraph, the other, the Planetary Camera (PC) of the *Hubble Space Telescope*. Together with the redetermined astrometric orbit and parallax, these yield new estimates of the component masses. The derived masses are $1.497 \pm 0.037\ M_\odot$ for the primary and $0.602 \pm 0.015 M_\odot$ for the white dwarf secondary. These mass values are heavily weighted by the PC separation measurement, which, while being somewhat discordant with the ground-based measures, we argue is more precise and more accurate and thus deserving of its greater weight. This stated, the long-standing discrepancy between previous determinations of the observed mass of Procyon A ($1.75\ M_\odot$) and the value supported by stellar evolution models ($1.50\ M_\odot$) appears to be reconciled.

Key words: astrometry — stars: individual (Procyon)

1. INTRODUCTION

The Procyon binary system (α CMi = HR 2943) consists of an F5 IV–V primary and a white dwarf secondary in an approximately 40 year orbit. The mass of the F5 primary as determined from stellar evolution theory does not agree with the value derived astrometrically by Strand (1951), nor with a more recent determination by Irwin et al. (1992), who combined Strand's (1951) photographic measures with radial velocity data. Irwin et al. (1992) obtain $1.75 \pm 0.05\ M_\odot$. By contrast, stellar evolution models, such as those of Guenther & Demarque (1993), conclude that the mass of Procyon A must be significantly lower, $1.50 \pm 0.05\ M_\odot$, in order to match its observed luminosity and effective temperature.

We have undertaken to redetermine, astrometrically, the component masses of the Procyon system. The total binary mass is specified by Kepler's law and knowledge of the system's parallax, orbital period, and semimajor axis of the visual orbit (i.e., that of the secondary with respect to the primary). The component masses follow given the semimajor axis of the astrometric orbit (i.e., that of the primary with respect to the barycenter).

The parallax, period, and astrometric orbit can be determined from existing photographic plate material and precise measurement of the motion of the primary relative to an arbitrary reference frame of background stars. Knowing the astrometric orbit, the size of the visual orbit can then be deduced, in theory, from a single observation of the A-B separation. In practice, this is a very difficult observation for the Procyon double given the 5″ maximum separation and ∼10 mag difference in brightness! The two previous astrometric mass determinations relied solely (and critically) on the visual-micrometer measures, made by Aitken (1901) and Bardnard (1909, 1912) at the turn of the century, to set the scale of the visual orbit. We see this as a potential source of error based on our experience with other "difficult" double stars and systematic differences between visual and speckle observations, for example. Instead, we determine the visual orbit scale based on two modern separation measurements: one using a ground-based coronagraphic instrument, the other utilizing the Wide Field Planetary Camera 2 (WFPC2) of the *Hubble Space Telescope* (*HST*).

In a previous astrometric study of Procyon, Strand (1951) used Gaertner long-screw measures of approximately 200 photographic exposures from the Yerkes Observatory 40 inch (1.0 m) and McCormick Observatory 26 inch (0.67 m) refractors, spanning the years 1915–1949, to derive the astrometric orbital elements and parallax of the system. Strand (1951) also derived the parallax from radial velocity measures and a comparison of these with the astrometric orbit. These parallax values were averaged together with published values based on the Sproul, Yale University, and Van Vleck Observatories plate series to arrive at a final adopted absolute parallax of 0.″287 ± 0.″004. He then combined the astrometric orbit and parallax with the visual separation observations by Aitken and Barnard between 1897 and 1913 to set the scale of the visual orbit and derive

[1] Department of Astronomy, Yale University, P.O. Box 208101, New Haven, CT 06520-8101; girard@astro.yale.edu, jlee@astro.yale.edu, vanalten@astro.yale.edu.
[2] Center for Imaging Science, Rochester Institute of Technology, 54 Lomb Memorial Drive, Rochester, NY 14623-5604; ephpci@cis.rit.edu.
[3] Space Telescope Science Institute, 3700 San Martin Drive, Baltimore, MD 21218; gillil@stsci.edu, bond@stsci.edu.
[4] Current address: Department of Physics, Astronomy, and Geosciences, Towson University, Towson, MD 21252; kschaef@towson.edu.
[5] Department of Physics, Michigan Technological University, 1400 Townsend Drive, Houghton, MI 49931-1295; cftaclas@mtu.edu.
[6] Lunar and Planetary Laboratory, University of Arizona, Tucson, AZ 85721; rhb@lpl.arizona.edu.
[7] NASA Infrared Telescope Facility, P.O. Box 4729, Hilo, HI 96720; toomey@irtf.ifa.hawaii.edu.
[8] Department of Physics and Astronomy, Sharp Laboratory, University of Delaware, Newark, DE 19716-2570; harrys@strauss.udel.edu.
[9] Institut d'Astronomie et d'Astrophysique, Université Libre de Bruxelles, C.P. 226, Boulevard du Triomphe, B-1050 Brussels, Belgium; pourbaix@astro.ulb.ac.be.

individual masses. In this manner, Strand (1951) derived values of 1.74 and 0.63 $M_\odot$, respectively, for the primary and secondary component masses.

Irwin et al. (1992) reanalyzed Strand's (1951) plate measures and complemented these with absolute and relative radial velocity measures. Using their combined astrometric/radial velocity orbit solution and the visual separation measures of Aitken and Barnard, Irwin et al. (1992) derive values of $M_A = 1.751 \pm 0.051\ M_\odot$ and $M_B = 0.622 \pm 0.017\ M_\odot$ for the component masses.

In this study, we redetermine the orbit of the Procyon system based solely on astrometric measures, using an extended collection of plates spanning 83 years. The plate material and measurements are described in § 2, and the reduction of these measures to yield the astrometric orbit and parallax of the system is detailed in § 3. In § 4, two modern separation measures are presented, and these are utilized in § 5 to deduce the visual orbit and the component masses. These values are discussed and compared with previous observational determinations, primarily that of Irwin et al. (1992). We conclude with a summary of our results and an update on an ongoing program to observe the Procyon system with the WFPC2.

2. PHOTOGRAPHIC MEASURES

Suitable plate material was gathered from the plate archives of six different observatories for measurement with the Yale PDS microdensitometer. In total, 266 plates spanning 83 years and containing 819 sets of exposures were measured, although roughly 25% of these did not contribute to the final astrometric solutions. The rather large fraction of discarded measures is a result of the large range in quality of the photographic plates and our decision to measure all available plates, even those with obviously unacceptable images. (Based on our past experience, the astrometric quality of a plate does not *always* correlate with a subjective assessment of the image quality.) Preliminary plate-pair and multiple-plate solutions were used to identify and discard flawed and discordant plates. Table 1 summarizes all of the photographic material. Strand (1951) made use of the pre-1950 Yerkes and McCormick Observatories plate material.

The various plate series employed a variety of techniques for reducing the effective magnitude of Procyon. These are also listed in Table 1. The magnitude reduction is necessary in order to simultaneously produce measurable images of Procyon and a sufficient number of fainter stars to form the reference frame. For those plates with measurable central and second-order diffraction-grating images of Procyon, the positional differences between the two orders were used to derive a linear magnitude equation correction, which was applied to all images on the plate. (See Girard et al. 1998 for a discussion of magnitude equation and the use of grating images in providing a correction.)

Image centers were determined using the standard Yale two-dimensional Gaussian fitting software. The white dwarf secondary is not visible on any of the photographic material, being hopelessly blended into the primary's image. In fact, the measured photocenter was adopted as the position of the primary itself since, with a 10 mag difference in brightness between components, the offset between primary and photocenter was totally negligible.

3. ASTROMETRIC ORBIT AND PARALLAX

The superior quality of the US Naval Observatory (USNO) plates and the different timescales for the parallactic and orbital motions suggested a two-step reduction strategy. All of the various plate series would be used in the orbit solution, which, in an iterative procedure, would also yield a rough, "all-plate–series" parallax. Once the final orbital elements were obtained, the USNO plate measures would be precorrected for this orbital motion and a final parallax would be derived based only on the USNO plate series.

The parallax solution was determined by weighted least-squares fitting of (x, y) as a function of time. The weights are based on the image-centering error calculated by the two-dimensional Gaussian fitting code. The Yale parallax-fitting software was modified to allow the subtraction of a "known" orbital motion, prior to fitting for parallax and proper motion. The "solved-for" parallax and proper motion could then be subtracted and the "known" orbit added back into the residuals, which were then passed into a separate routine that solved for improved orbital elements, again by a nonlinear least-squares method. This procedure was iterated until convergence, and the resulting orbital elements were adopted as final. Uncertainty estimates were derived from the curvature of the χ^2 surface in the vicinity of the final solution, one parameter at a time, while allowing the remaining parameters to be free, of course. Once these final orbital elements were determined, they were used to make a final parallax solution using only the USNO plate series, which spans roughly five years.

Trial orbit/parallax solutions were made using both weighted and unweighted least-squares methods, with the unweighted solution being adopted because the plate-to-plate variations are probably dominated by unpredictable systematic differences (e.g., guiding-error differences). In any

TABLE 1

PHOTOGRAPHIC MATERIAL

Telescope	Epoch Span	N_{plate}	N_{exp}	Magnitude Reduction	Reduction Technique
Sproul 24 inch (0.61 m)	1912–1914	4	12	9.0	Rotating sector
McCormick 26 inch	1915–1916	9	27	7.5	Rotating sector
	1923–1971	58	195	8.9	Neutral-density filter + rotating sector
Yerkes 40 inch	1918–1948	46	148	10.0	Rotating sector
	1949–1957	38	108	10.0	Rotating sector + objective grating
Van Vleck 20 inch (0.51 m)	1924–1929	26	50	9.1	Rotating sector
	1929–1933	11	48	9.1	Neutral-density filter + rotating sector
	1995	4	12	9.0	Rotating sector + objective grating
Yale 26 inch (0.66 m)	1929–1933	21	80	10.5	Rotating sector + objective grating
USNO 61 inch (1.55 m) reflector.....	1985–1990	49	139	12.0	Neutral-density filter

event, the two solutions yielded orbital elements that agreed to within their estimated errors. A large number of high-residual outliers were discarded from the all-plate–series solution, leaving 599 exposures for the orbit determination. Figure 1 shows the final astrometric orbit fit to the plate measures with parallax and proper motion subtracted.

Table 2 lists the derived elements of the astrometric orbit, along with those obtained by Strand (1951) and by Irwin et al. (1992). The Irwin et al. values are those of their combined astrometric and radial velocity solution, extracted from their Table 6. The errors listed in the first column are formal errors from the least-squares fit but are to be viewed with caution because of the large amount of data trimming performed. For several of the elements, our values differ significantly from those of Irwin et al. (1992), notably in semimajor axis, eccentricity, and period, in which there is actually better agreement with Strand (1951).

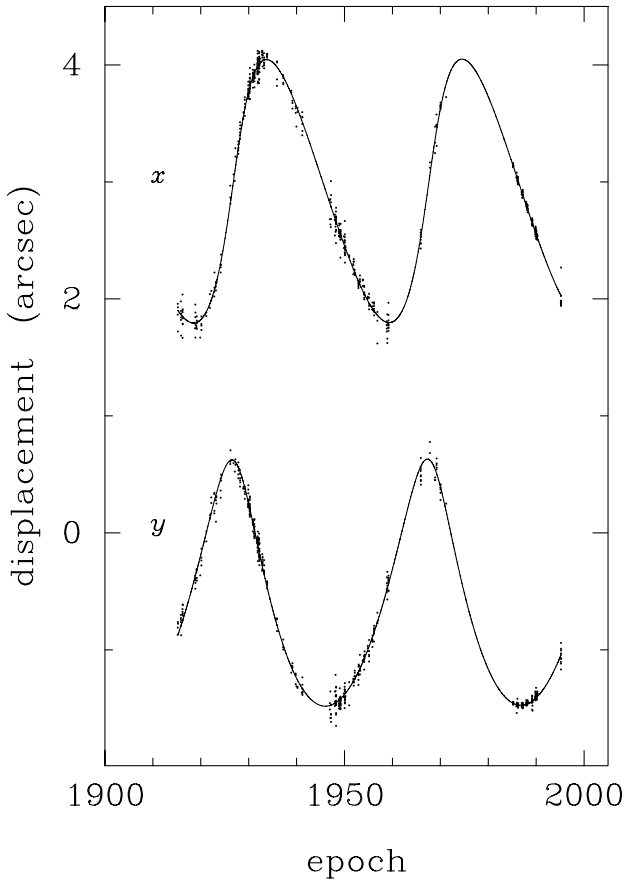

FIG. 1.—Astrometric-orbit determination for Procyon A. The points indicate PDS measures of individual exposures and the curve shows the least-squares solution for the orbit. The plate measures have been transformed to a common reference system. Only those measures which contributed to the orbit solution are included. The x- and y-coordinates are nominally aligned with right ascension and declination.

As described above, the final orbital elements were then applied to the individual plate measures, and the parallax was determined first with all of the plate series and finally with just the USNO plates. These relative parallaxes are transformed to absolute by applying a correction based on the mean magnitude of the reference stars (see van Altena, Lee, & Hoffleit 1995 for details). The resulting absolute parallax estimates are presented in Table 3, along with that of the USNO result (Harrington et al. 1993) for their own plates and the value obtained by the *Hipparcos* mission (ESA 1997). Our value is consistent with that of USNO (within the combined uncertainties), with a formal improvement in accuracy to 1.5 milliarcseconds. This can be attributed to the use of the PDS to measure these excellent plates.

The *Hipparcos* parallax differs from our value by approximately 1.6 times the combined uncertainties and, in fact, is in closer agreement with the USNO value. In both the USNO and *Hipparcos* investigations, the observation baseline was short enough that an orbit was assumed, instead of being solved for. In the case of the *Hipparcos* reductions, the orbital elements assumed were those of Irwin et al. (1992). What would be the effect on the parallax derived from the *Hipparcos* data had one assumed the revised orbital elements presented here? To answer this question, we rederived the *Hipparcos* astrometric solution from the intermediate astrometric data that accompany the *Hipparcos* catalog CD version and that are also available on the *Hipparcos* Web site.[10] The revised parallax solution was performed using the procedures and software described by Pourbaix & Jorissen (2000). The effect of adopting the new orbital parameters was minimal, decreasing the derived parallax by a mere 0.1 mas. As one might expect, the effect

[10] At http://astro.estec.esa.nl/Hipparcos.

TABLE 2

ASTROMETRIC ORBIT ELEMENTS OF PROCYON

Element	Strand (1951)	Irwin et al. (1992)	Present Study
Semimajor axis, α_A (arcsec)	1.217	1.179	1.232
	±0.002	±0.011	±0.008
Eccentricity, e	0.40	0.365	0.407
	...	±0.008	±0.005
Inclination, i (deg)	35.7	31.9	31.1
	±0.2	±0.9	±0.6
Angle of node, Ω (deg)	104.3	104.8	97.3
	±0.3	±1.5	±0.3
Longitude of periastron, ω (deg)	89.8	88.8	92.2
	±0.3	±2.0	±0.3
Period, P (yr)	40.65	40.38	40.82
	...	±0.15	±0.06
Periastron passage, T (yr)	1927.6	1967.86	1967.97
	(1968.3)	±0.16	±0.05

TABLE 3

TRIGONOMETRIC PARALLAX OF PROCYON

Source	Plate Material	π_{rel} (arcsec)	m_{pg}(ref)	Correction to Absolute	π_{abs} (arcsec)
Present study.....	Combined	0.2792	10.0	0.0027	0.2819 ± 0.0032
	USNO series	0.2819	13.0	0.0013	0.2832 ± 0.0015
USNO	USNO series	0.2850	13.1	0.0013	0.2864 ± 0.0024
Hipparcos.....	...	...	...	...	0.28593 ± 0.00088

on the derived absolute proper motion was more substantial. Using the Irwin et al. (1992) orbit, we obtain $\mu_\alpha \cos\delta = -716.56 \pm 0.88$ mas yr^{-1}, $\mu_\delta = -1034.56 \pm 0.38$ mas yr^{-1}, virtually identical to the published *Hipparcos* result. However, adopting our revised values for the orbit yields $\mu_\alpha \cos\delta = -710.95 \pm 0.88$ mas yr^{-1}, $\mu_\delta = -1020.49 \pm 0.38$ mas yr^{-1}. The difference is significant, although it is difficult to judge which of the two values is more correct: precise, ground-based, photographic measures of Procyon's motion with which one might compare are relative and not absolute, including that which we derive in our parallax/orbit solution.

4. A-B SEPARATION MEASURES

4.1. CoCo *Observations*

The infrared cold coronagraph known as CoCo is described by Wang et al. (1994). It features selectable, apodized focal-plane masks. Initial tests of the instrument were made in 1995 February with the 3 m telescope of the NASA Infrared Telescope Facility (IRTF) at Mauna Kea, Hawaii, using the IRTF NSFCAM as a detector. Among the first exposures recorded were two *K*-band images of Procyon, one of which is presented in Figure 2. The white dwarf secondary is clearly visible in the northeast quadrant

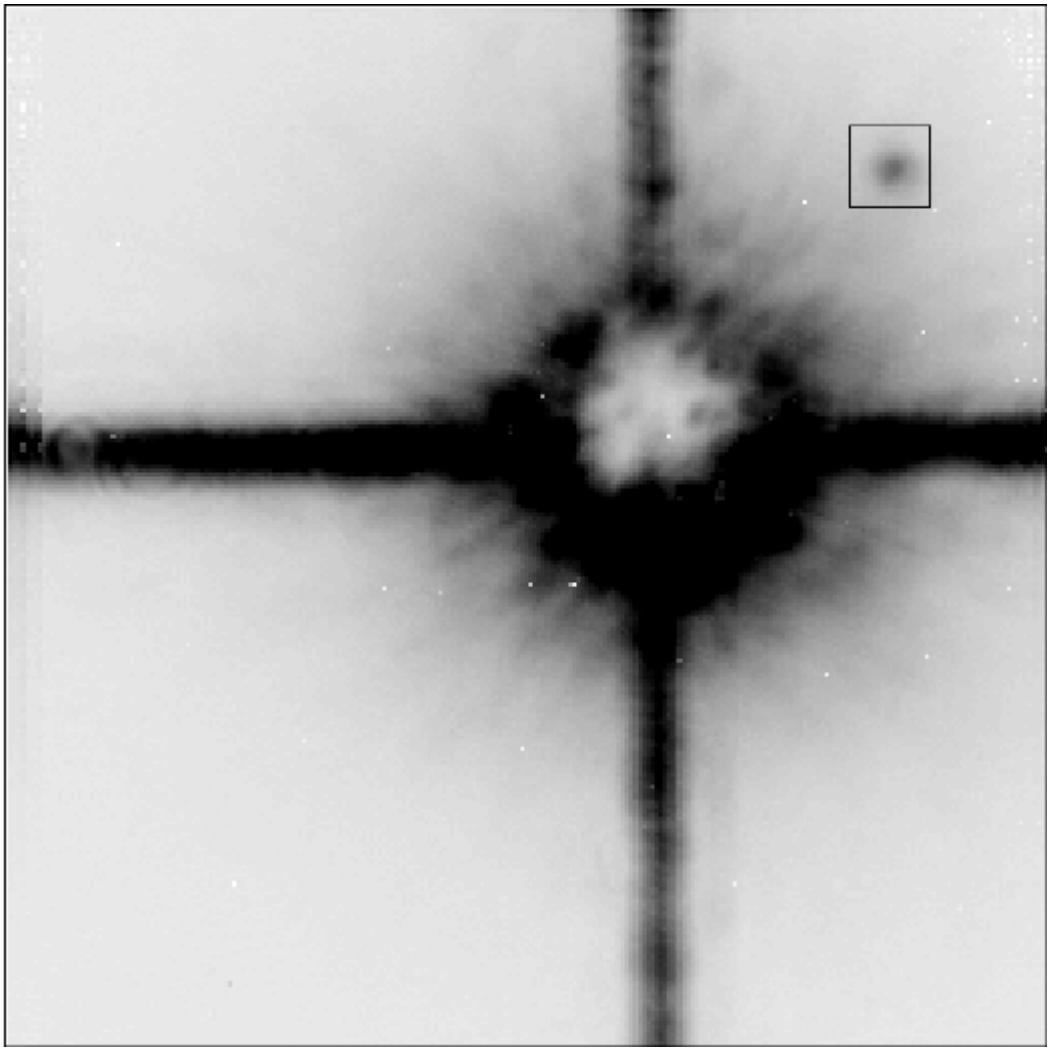

FIG. 2.—CoCo coronagraph image of Procyon A-B taken 1995.09 with the NASA IRTF 3 m telescope. This is a 10 s exposure taken in *K* band with the primary positioned behind the apodized, occulting mask. The image of the white dwarf secondary is indicated.

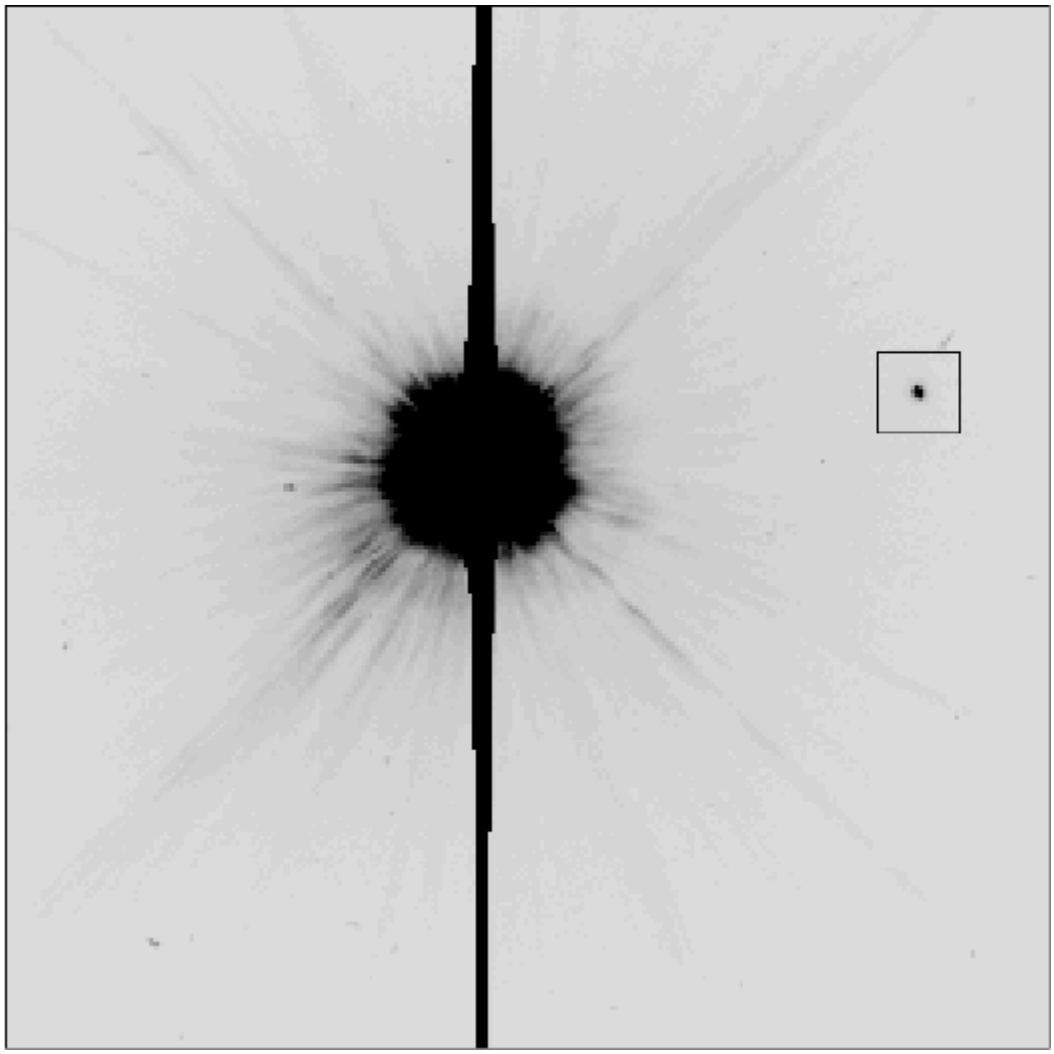

FIG. 3.—WFPC2 PC image of Procyon A-B taken 1995.18 with the *HST*. This 160 s exposure was with the F218W filter. The inner 256 × 256 portion of the PC frame is shown. The position of the primary was determined from a 0.11 s exposure taken moments earlier.

of the frame, well separated from the occulted primary. We have calculated the A-B separation based on this frame, as well as another similar exposure from the same night. The position of the primary was determined by modeling the diffraction spikes beyond the apodized portion of the mask. The secondary's position was determined by fitting an elliptical paraboloid to its image, fitting only those pixels above an appropriate threshold. The mean separation from the two frames, at epoch 1995.09, was found to be 90.4 ± 0.9 pixels. This includes a correction of $+0.3$ pixels to offset the bias from the sloping background at the position of the secondary image, caused by the wings of the primary image. The 0.9 pixel uncertainty is dominated by the fit to the overexposed diffraction spikes of the primary. It was estimated from the scatter in the fitted positions as derived using various fitting techniques and is consistent with the difference in separation values, 0.6 pixels, derived from the two separate frames.

The pixel scale of the CoCo-NSFCAM combination is not well known, and thus we have deduced a nominal scale based on four short exposures of γ Vir (STF 1670) observed in 1995 March with the same instrument. Unfortunately, the orbit of this bright ($V_A = V_B = 3.4$) binary is also not well known, having been last updated (coincidentally) by Strand (1937) in 1937. Thus, we have undertaken a redetermination of its visual orbit based on all available measures contained in the Washington Double Star (WDS) Catalog (Worley & Douglass 1996),[11] supplemented by an additional speckle interferometric measure made in 1996 February as part of the Yale/San Juan Double Star Project (Horch et al. 1996). This final observation strengthens the relevant ephemerides separation and position angle (P.A.) of γ Vir at 1995.249, making it a true interpolation. Our new orbit solution for γ Vir leads to a CoCo-scale estimate of $0\farcs0566 \pm 0\farcs0006$ pixel^{-1}. Details of this calculation, including the new visual orbit solution of γ Vir, are described in the Appendix. With the above value for the instrument scale, the CoCo separation of Procyon A-B becomes $5\farcs12 \pm 0\farcs07$ (1995.09; P.A. $= 41\fdg0 \pm 1\fdg0$).

4.2. *HST WFPC2 Observations*

In 1995 March, a series of observations were made of Procyon using the WFPC2 Planetary Camera (PC) of the *HST* with the intention of accurately measuring the A-B separation. One such PC frame, a 160 s exposure taken with the F218W filter, is shown in Figure 3. In it, the secondary is readily measurable and well separated from the heavily

[11] Electronic version available at http://aries.usno.navy.mil/ad/wds.

saturated primary image. The position of the primary can be determined from a 0.11 s exposure taken several minutes earlier at the same telescope pointing. The guiding stability of the telescope is expected to be no worse than 0.″005 over the course of several minutes, and we have confirmed this value based on a set of 10 pairs of archive images taken under similar circumstances, i.e., repeated exposures several minutes apart.

After experimenting with Gaussian fitting and theoretical point-spread function (PSF) fitting, the method we have chosen for position determination is cross-correlation between the primary image in the short exposure and the secondary image in the long exposure. Integer-offset cross-correlation values were interpolated using a bicubic function to obtain the final, fractional pixel displacement of image B relative to A. The resulting (interpolated) cross-correlation value of 0.94 indicates the PSFs of the two images are good matches to one another. The resulting A-B separation is 108.63 pixels with an estimated uncertainty of 0.2 pixels due to undersampling by the PC.

It is also possible to measure the separation entirely from the long exposure alone, keying on the diffraction spikes of the saturated primary image to determine its position. Doing so yields a separation value consistent with that based on the cross-correlation of long and short exposures, but with an estimated error approximately twice as large. Thus, we choose to adopt the separation value based on the cross-correlation of long and short exposures, as described above.

The scale and optical field-angle distortion of the PC, including its wavelength dependence, has been characterized by Holtzman et al. (1995). Geometric distortion is small over the central 100 pixels, but it is not zero. Sources are closer than they appear, and the correction to the separation at the positions of images A and B is -0.07 pixels. The chip-center plate scale is $0.''04557 \pm 0.''00002$ pixel^{-1} at F555W, and the relative scale at F218W to F555W is 0.99737 ± 0.0002. Thus, the color-corrected plate scale is $0.''04545$ pixel^{-1}, and the distortion-corrected separation of 108.56 pixels yields a final A-B separation value of $4.''934 \pm 0.''011$ at epoch 1995.177. The largest sources of uncertainty are pixel undersampling ($0.''009$) and possible guiding error ($0.''005$), while uncertainties in the PC plate scale, distortion, color correction, and possible bias from the sloping background due to image A are all estimated to be less than $0.''002$ each.

The derived position angle is $42.°8 \pm 0.°2$, based on the *HST* fine guidance sensors and the known guide star positions. This position angle measurement is in excellent agreement with that implied by the astrometric orbit specified in Table 2, which predicts a value of $42.°86$ at this epoch.

The separation, however, disagrees with that measured by the CoCo instrument, at the 2.6 σ level. The difference corresponds to 4 PC pixels, much larger than one could expect from an as yet unaccounted for error in the PC measure. Having more thoroughly investigated the astrometric properties of the PC, including numerous tests involving archival images, we feel the discrepancy is more likely due to the CoCo measure with its appropriately larger error estimate.

5. VISUAL ORBIT AND COMPONENT MASSES

Adopting the astrometric orbit elements given in Table 2 and the two separate estimates of the A-B separation from above, the semimajor axis of the visual orbit can be derived. Combined with the new determination of the parallax, the component masses follow. We calculate visual orbits and masses based on the CoCo and WFPC2 results separately. These are given in Table 4, along with the findings of Strand (1951) and Irwin et al. (1992) for comparison. Error estimates, when available, are listed just below the values. Note that the values extracted from Irwin et al. (1992) are from their combined astrometric and radial velocity solution (their Table 6).

Both of the new estimates of M_A are significantly lower than the previous determinations. In particular, the value based on the WFPC2 measurement is in good agreement with the predictions of the stellar modelers, 1.5 $M_\odot$. The CoCo-based value, with its larger formal uncertainty, falls between the stellar model prediction and the value measured by Irwin et al. (1992).

The difference between the current results and those of Strand (1951) and Irwin et al. (1992) is due in part to their reliance on the visual separation measures. In Figure 4, we show the various separation measures as a function of time, along with the CoCo-based and WFPC2-based visual orbits just derived. The visual micrometer observations of Aitken and Barnard are indicated by filled circles. The triangle represents another ground-based coronagraphic measure by Walker et al. (1994) using the Canada-France-Hawaii Telescope 3.6 m telescope. They find a separation of $5.''2$ and position angle of $36.°3$ at epoch 1992.72 but do not estimate errors[12] or discuss the calibration of the camera scale. It is difficult to judge the significance of the better agreement of the Walker et al. (1994) result with our own coronagraphic measure, as opposed to our space-based measure. As an indication of the random error of a visual observation, consider the 1986 measure by Worley (1989). The value of $5.''1$ was the average of two nights' measures of $4.''8$ and $5.''4$.

Figure 5 shows the early observations in more detail and also includes the orbits derived by Strand (1951) and Irwin et al. (1992). Near maximum separation (i.e., epoch 1907), the two new orbit determinations bracket the previous ones, even though both of the new orbits correspond to smaller semimajor axis values as well as to lower estimates of M_A. Clearly, the differences in the orbital elements are important, not just the orbit scale. The disagreement in overall orbit shape with that of Irwin et al. (1992) is somewhat disturbing. While our astrometric data are unquestionably of higher quality and better phase coverage than that available to Irwin et al. (1992), their use of absolute radial velocity data and precise relative radial velocity data in their combined solution should have compensated. While a rigorous investigation combining our astrometric data with existing radial velocity measures may shed light on this discrepancy, we have chosen to limit this present study to astrometric data alone.

Returning to the component masses, we feel confident that we have considered all possible influences on the WFPC2 pixel scale and consequent uncertainty estimate of the WFPC2-based separation measure. Therefore, the respective error estimates of the CoCo-based and WFPC2-

[12] G. A. H. Walker (1998, private communication) reports that the measured separation was actually $5.''25$ with an estimated precision of $0.''01$, although the unresolved question of accuracy versus precision dissuaded them from quoting an uncertainty in their paper.

TABLE 4

VISUAL ORBIT ELEMENTS AND COMPONENT MASSES OF PROCYON

ELEMENT	STRAND (1951)	IRWIN ET AL. (1992)	PRESENT STUDY	
			CoCo	WFPC2
Semimajor axis, α (arcsec)	4.548	4.496	4.405	4.271
	...	$\pm$0.060 [a]	$\pm$0.070	$\pm$0.032
Absolute parallax, π (arcsec)	0.287	0.2864 [b]	0.2832	
	$\pm$0.004	$\pm$0.0023	$\pm$0.0015	
Orbital period, P (yr)	40.65	40.38	40.82	
	...	$\pm$0.15	$\pm$0.06	
Total mass, M_{sum} ($M_\odot$)	2.37 [c]	2.373	2.258	2.059
		$\pm$0.110	$\pm$0.113	$\pm$0.057
Mass of component A, M_A ($M_\odot$).....	1.74	1.751	1.626	1.465
	...	$\pm$0.087	$\pm$0.082	$\pm$0.041
Mass of component B, M_B ($M_\odot$)	0.63	0.622	0.632	0.594
	...	$\pm$0.023	$\pm$0.032	$\pm$0.017

[a] Irwin et al. 1992 suggest that a conservative uncertainty estimate, 3 times the formal uncertainty in α, is appropriate considering the heavy trimming and possible bias in the visual separations. Given here is the conservative 3 times uncertainty estimate of Irwin et al., which is propagated through to the uncertainty estimates of the derived masses.

[b] Irwin et al. 1992 adopt the USNO parallax value for the purpose of mass determination.

[c] Strand's 1951 derived values for the masses are not precisely consistent with his values for α, π, and P.

based mass determinations can be used to yield weighted averages of the component mass values. Doing this, our final, best values of the Procyon masses are 1.497 ± 0.037 $M_\odot$ for the primary and 0.602 ± 0.015 $M_\odot$ for the white dwarf secondary.

This value of M_A reconciles the disagreement with stellar models described by Guenther & Demarque (1993). They find that assuming solar composition and a parallax of 0".287, the luminosity and effective temperature of Procyon are best fitted by a model with mass 1.50 ± 0.05 $M_\odot$. This was discordant with the then recent measure by Irwin et al. (1992) of $M_A = 1.751 \pm 0.051$ $M_\odot$ (± 0.087 $M_\odot$, adopting the more conservative error estimate of Irwin et al. 1992). Note that our value for the combined mass, 2.099 $M_\odot$, represents a 12% decrease from the value of Irwin et al. (1992). Of this, -13% is attributable to the change in α; -2% is due to the revision in P; and $+3\%$ results from our somewhat lower value of parallax.

Finally, we note that the value of $M_B = 0.602$ $M_\odot$ is slightly higher than the average (0.587 $M_\odot$) and the mode (0.50–0.55 $M_\odot$) of the mass distribution of field white dwarfs (Bragaglia, Renzini, & Bergeron 1995). This is not surprising since, being descended from a progenitor star of mass greater than 1.5 $M_\odot$, Procyon B would be expected to have a higher than average mass.

6. SUMMARY

Drawing on the plate collections of five observatories, including roughly 600 exposures spanning 83 years, we have redetermined the parallax and astrometric orbit of the Procyon binary. The resulting parallax value, 0".2832 $\pm$ 0".0015, is somewhat lower than the value obtained by

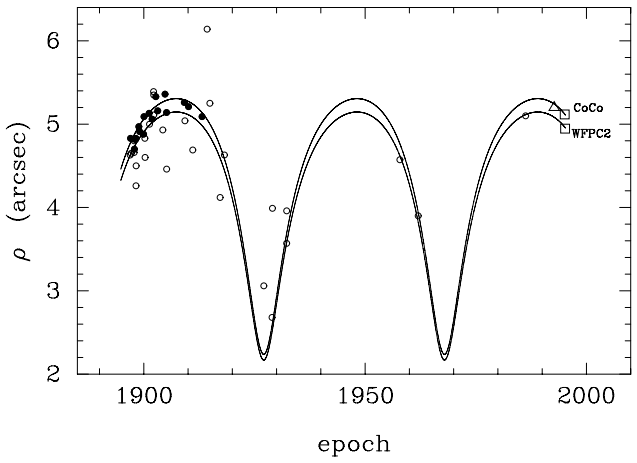

FIG. 4.—Procyon A-B separation measures as a function of epoch. The circles indicate visual micrometer measures, the filled circles being the more uniform (and presumably more reliable) measures by Aitken and Barnard. The triangle shows the coronagraphic measurement by Walker et al. (1994). The squares represent the measures presented here: the CoCo coronagraph measure and the *HST* WFPC2 result. The curves show the visual orbit solutions that result from combining each of these two measures with the derived, astrometric orbit elements.

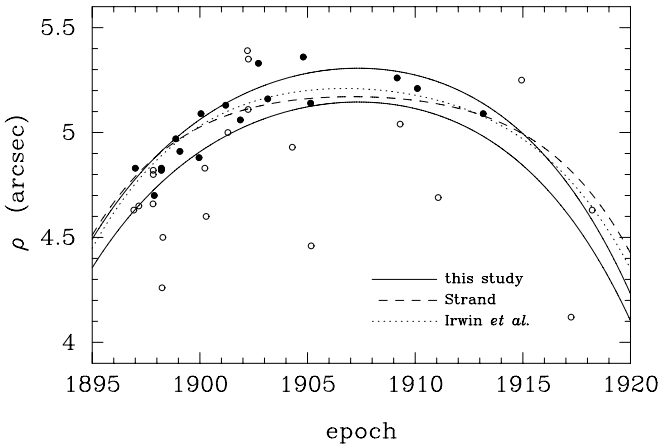

FIG. 5.—Similar to Fig. 4, but showing the early visual observations in greater detail. The published visual orbit solutions of Strand (1951) and Irwin et al. (1992) have also been included, indicated by the dashed and dotted curves, respectively. The solid curves are the two solutions from this study. The CoCo-based curve lies above the one based on the WFPC2 measure.

Hipparcos, 0″.28593 ± 0″.00088. The astrometric orbit differs at a significant level from that of the previous, most recent determination, that of Irwin et al. (1992). The difference in astrometric orbit parameters (*Hipparcos* reductions adopted the Irwin et al. 1992 orbit) cannot account for the difference in parallax findings.

In order to derive component masses for the system, two distinct measurements have been made of the A-B separation: one employing a ground-based coronagraphic camera (CoCo); the other, the WFPC2 PC of *HST*. Not surprisingly, the WFPC2 measure is more precise and, we feel, more accurate, and thus we have allowed it to dominate the weighted-average separation value adopted here. This separation, when combined with the new astrometric orbit, leads to derived masses of $1.497 \pm 0.037\ M_{\odot}$ for the primary and $0.602 \pm 0.015\ M_{\odot}$ for the white dwarf secondary. This new value for the primary is substantially lower (∼12%) than previous astrometric and combined astrometric/radial velocity–based determinations, which assumed visual separation measures to set the scale of the orbit. If correct, the new value of M_A resolves the long-standing discrepancy between the measured mass and that predicted by stellar evolution theory.

A "long-term" program to monitor Procyon with the *HST* PC has been initiated by some of the authors in the hope of obtaining high-precision separation and position-angle measures over a sufficient fraction of the 40 year orbit. It is hoped that this program will enable us to eventually confirm and refine the ground-based astrometric orbit determination with an entirely space-based measure of the visual orbit.

We are grateful to the directors of the McCormick, Sproul, Van Vleck, US Naval, and Yerkes Observatories for allowing us to borrow the invaluable plate material that made this project possible. We also thank Edward Weis of the Van Vleck Observatory for fulfilling our request to extend the Van Vleck series with a set of 1995 plates. One of us (T. M. G.) wishes to acknowledge David Guenther for bringing the Procyon mass dispute to our attention and Alan Irwin for very helpful comments on an early version of this paper. We would also like to thank the director of the Space Telescope Science Institute for a small grant of discretionary time on *HST* to add short exposures to an existing General Observer program of one of us (H. L. S.) to study Procyon B. This work was supported in part by funds from the National Science Foundation, including a grant from the AAS Research Experiences for Undergraduates program. Portions of this research are based on observations made with the NASA/ESA *HST*, obtained at the Space Telescope Science Institute, which is operated by the Association of Universities for Research in Astronomy, Inc., under NASA contract NAS 5-26555. This research has also been funded, in part, by ESA through an ESA Prodex grant, contract 13317-98-NL-VJ.

APPENDIX

ASTROMETRIC ORBIT OF γ VIRGINIS

The bright binary γ Vir (STF 1670) was observed with CoCo-NSFCAM on 1995.249 for the purpose of calculating the scale of that instrument. Four *K*-band exposures were taken, with the binary positioned on different regions of the detector, but not obscured by the occulting mask. Each exposure consisted of 10 0.1 s snapshots co-added, resulting in irregularly shaped star images, presumably due to speckle imaging! The binary separation was therefore measured by forming the autocorrelation of each image and fitting the secondary peak of the autocorrelated image. Averaging the results from the four images yielded an instrument separation of 38.53 ± 0.17 pixels, where the error estimate is the standard deviation of the four measures.

TABLE 5

VISUAL ORBIT OF γ VIRGINIS

Element	Strand (1937)	Present Study
Semimajor axis, α (arcsec)	3.746	3.619 ± 0.012
Eccentricity, *e*	0.881	0.8781 ± 0.0025
Inclination, *i* (deg)	146.05	150.38 ± 0.35
Angle of node, Ω (deg)	31.78	32.88 ± 0.18
Longitude of periastron, ω (deg)	252.88	252.62 ± 0.16
Period, *P* (yr)	171.37	168.93 ± 0.43
Periastron passage, *T* (yr)	1836.43	1836.45 ± 0.19

The actual angular separation of the binary could not be accurately derived from the existing orbit solution (Strand 1937), and thus all available separation measures were extracted from the WDS Catalog, 1081 observations spanning 172 years, in order to redetermine the visual orbit. An additional observation was added; a speckle interferometric measurement on 1996.118 was made as part of the Yale/San Juan Double Star Project. Several weighting schemes were tested, primarily changing the weights of the two speckle

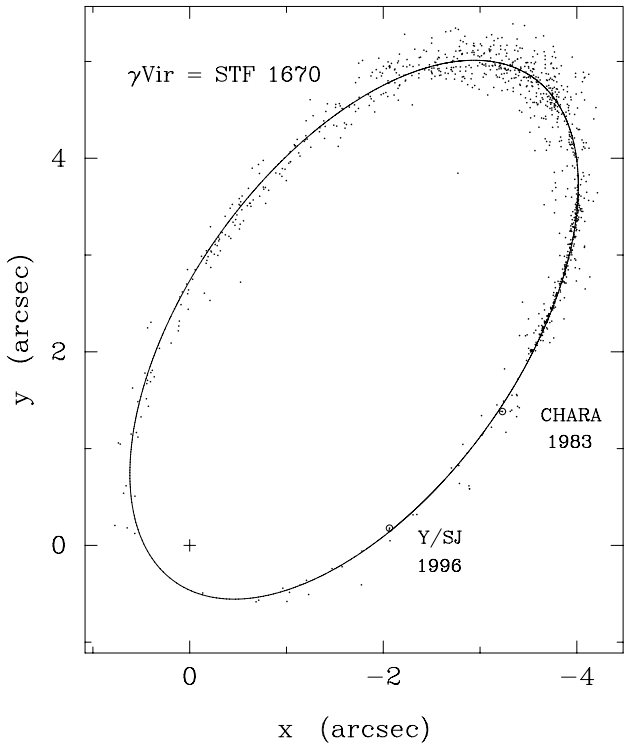

FIG. 6.—Visual orbit of γ Vir as derived in this study. The points represent primarily visual and photographic measures. The measures made using speckle interferometry are circled and labeled. An accurate separation of γ Vir A-B was needed to calibrate the scale of the CoCo coronagraph.

points relative to the visual observations (there was a 1983 CHARA speckle observation in addition to the Yale/San Juan one). It was decided that for this widely separated, equal-brightness binary, the speckle measures were not necessarily more accurate, and thus a final solution using equal weights for all observations was adopted. Table 5 summarizes the resulting orbit solution for γ Vir, alongside the previous determination by Strand (1937). Figure 6 illustrates the new orbit fit.

From this orbit solution, the 1995.249 separation of γ Vir is $2''.182 \pm 0''.010$, where the error is estimated from the variation over a number of trial solutions employing different weighting schemes and using a range of (reasonable) data-trimming limits. Combined with the pixel separation, this leads to a CoCo-NSFCAM scale of $0.0566 \pm 0''.0006$ pixel^{-1}. The orientation of the detector was also found to coincide with the celestial system to within $\pm 1°$.

We also note that γ Vir remains on the observing lists of both the USNO and Yale/San Juan speckle interferometry programs. Inclusion of these accumulating measures will soon allow a definitive redetermination of the orbit of γ Vir.

REFERENCES

Aitken, R. G. 1901, Lick Obs. Bull., 1(11), 66
Barnard, E. E. 1909, Astron. Nachr., 182, 13
———. 1912, AJ, 27, 104
Bragaglia, A., Renzini, A., & Bergeron, P. 1995, ApJ, 443, 735
ESA. 1997, The Hipparcos and Tycho Catalogues (ESA SP-1200) (Noordwijk: ESA)
Girard, T. M., Platais, I., Kozhurina-Platais, V., van Altena, W. F., & López, C. E. 1998, AJ, 115, 855
Guenther, D. B., & Demarque, P. 1993, ApJ, 405, 298
Harrington, R. S., et al. 1993, AJ, 105, 1571
Holtzman, J., et al. 1995, PASP, 107, 156
Horch, E. P., Dinescu, D. I., Girard, T. M., van Altena, W. F., Lopez, C. E., & Franz, O. G. 1996, AJ, 111, 1681
Irwin, A. W., Fletcher, J. M., Yang, S. L. S., Walker, G. A. H., & Goodenough, C. 1992, PASP, 104, 489
Pourbaix, D., & Jorissen, A. 2000, in preparation
Strand, K. A. 1937, Ann. Sternw. Leiden, 18, 37
———. 1951, ApJ, 113, 1
van Altena, W. F., Lee, J. T., & Hoffleit, E. D. 1995, The General Catalogue of Trigonometric Stellar Parallaxes (4th ed.; New Haven, CT: Yale Univ. Obs.)
Walker, G. A. H., Walker, A. R., Racine, R., Fletcher, J. M., & McClure, R. D. 1994, PASP, 106, 356
Wang, S., Owensby, P. D., Toomey, D. W., Brown, R. H., Stahlberger, W. E., Cavedoni, C. P., Hua, R., & Ftaclas, C. 1994, Proc. SPIE, 2198, 578
Worley, C. E. 1989, Publ. US Nav. Obs., 25, 71
Worley, C. E., & Douglass, G. 1996, The Washington Double Star Catalog (Washington: US Nav. Obs.)